Synthesis and Characterization of a New Microporous Material. 1. Structure of Aluminophosphate EMM-3

Mobae Afeworki, Douglas L. Dorset, Gordon J. Kennedy, and Karl G. Strohmaier*

ExxonMobil Research & Engineering Company, 1545 Rt. 22 East, Annandale, New Jersey 08801

Received September 28, 2005. Revised Manuscript Received December 21, 2005

Molecular sieves are extensively used in the chemical and petrochemical industry as catalysts, absorbents, and ion exchangers. New molecular sieve structures have the potential to improve the performance of these materials. We have discovered a new microporous material, EMM-3, prepared in both aluminophosphate and silicoaluminophosphate compositions by use of *N*,*N*,*N*,*N*′,*N*′,*N*′-hexamethyl-1,6-hexanediammonium as a template at 160 °C in 20 h. The structure of EMM-3 has been solved and refined from powder data by use of synchrotron X-ray radiation. The unit cell for the calcined AlPO form of EMM-3 has monoclinic space group symmetry, *I*2/*m*11, with cell dimensions $a = 10.3132(2)$, $b = 12.6975(3)$, and $c = 21.8660(4)$ and $\alpha = 89.656(1)°$. The microporous structure contains 12-ring, sinusoidal, unidimensional channels with pore openings of 6.1 × 6.5 Å. This new framework contains two *new* building chains, not observed in other known framework structures. The ^{31}P and ^{27}Al NMR spectra of the calcined/dehydrated form are in agreement with a fully connected tetrahedral structure containing five unique phosphorus and five unique aluminum atoms. The material is stable upon calcination and absorbs 9−10 wt % hydrocarbons.

Introduction

Microporous materials, including zeolites and silicoaluminophosphates, are widely used in the petroleum industry as absorbents, catalysts, catalyst supports, and ion exchangers. Their crystalline structures consist of three-dimensional frameworks containing uniform pore openings, channels, and internal cages of dimensions (<20 Å) similar to most hydrocarbons. One group of crystalline microporous compositions that displays the ion-exchange and adsorption characteristics of zeolites is the phosphates. This group includes aluminophosphates (AlPOs)[1] and silicon-substituted aluminophosphates (SAPOs).[2] These materials can have Al and P substitutions by B, Be, Mg, Ge, Zn, Fe, Co, Ni, etc., to form metal-substituted AlPOs and SAPOs, which are identified by the acronyms MeAPO or MeAPSO,[3] respectively.

Petroleum and petrochemical companies extensively use various microporous materials, such as faujasite, mordenite, and ZSM-5, as catalysts in many commercial applications, such as reforming, cracking, hydrocracking, alkylation, oligomerization, dewaxing, and isomerization. Any new material has the potential to improve the catalytic performance over those catalysts presently used. There are currently 165 International Zeolite Association Structure Commission approved microporous framework structures.[4] Each structure has unique pore, channel, and cage dimensions, which gives its particular properties as described above.

Most new microporous materials are synthesized with organic structure-directing agents (SDA), which can act as a template around which the growing framework can crystallize. These SDAs can be primary, secondary, or tertiary amines but are most often tetraalkylammonium cations such as tetraethylammonium and tetrapropylammonium hydroxides and halides. In some cases a particular SDA is very specific to directing the synthesis to only one material, while others, such as tetraethylammonium, can direct the synthesis to many different frameworks by variation of the synthesis composition and/or reaction conditions. The SDA, *N*,*N*,*N*,*N*′,*N*′,*N*′-hexamethyl-1,6-hexanediammonium cation (hexamethonium), has been found to induce the formation of a large number of zeolites such as EU-1,[5] ZSM-48,[6] SAPO-17,[7] IM-10,[8] ITQ-13,[9] ITQ-22, and ITQ-24.[10] We have discovered that this template can also form a new framework in the AlPO and SAPO systems. In this paper we describe the synthesis, characterization, and structure of the new crystalline, microporous aluminophosphate material EMM-3 (ExxonMobil Material No. 3) synthesized with the hexamethonium template.

Recent NMR techniques, such as multiple-quantum magic-angle spinning (MQMAS[11−13]) and MQ-selected hetero-

* To whom correspondence should be addressed: phone 908-730-2937; fax 262-313-2827; e-mail karl.g.strohmaier@exxonmobil.com.

(1) Wilson, S. T.; Lok, B. M.; Messina, C. A.; Cannan, T. R.; Flanigen, E. M. *J. Am. Chem. Soc.* **1982**, *104*, 1146.
(2) Lok, B. M.; Messina, C. A.; Patton, R. L.; Gajek, R. T.; Cannan, T. R.; Flanigen, E. M. *J. Am. Chem. Soc.* **1984**, *106*, 6062.
(3) Flanigen, E. M.; Lok, B. M.; Patton, R. L.; Wilson, S. T. In *New Developments in Zeolite Science and Technology*; Murakemi, Y., Iijima, A., Ward, J. W., Eds.; Elsevier: Amsterdam, 1986; p 103.
(4) International Zeolite Association Structure Commission, http://www.iza-structure.org/ as of December 16, 2005.
(5) Casci, J. L.; Lowe, B. M.; Whittam, T. V. In *Proceedings of the VI International Zeolite Conference*; Olson, D. H., Biseo, A., Eds.; Butterworth: Guildford, U.K., 1984; p 894.
(6) Schlenker, J. L.; Rohrbaugh, W. J.; Chu, P.; Valyocsik, E. W.; Kokotailo, G. T. *Zeolites* **1985**, *5*, 355.
(7) Valyocsik, E. W.; von Ballmoos, R. U.S. Patent 4,778,780, 1988.
(8) Mathieu, Y.; Paillaud, J. L.; Caullet, P.; Bats, N. *Microporous Mesoporous Mater.* **2004**, *75*, 13.
(9) Corma, A.; Puche, M.; Rey. F.; Sankar, G.; Teat, S. J. *Angew. Chem., Int. Ed.* **2003**, *42*, 1156.
(10) Sastre, G.; Pulido, A.; Castañeda, R.; Corma, A. *J. Phys. Chem. B* **2004**, *108*, 8830.

10.1021/cm052174r CCC: $33.50
Published on Web 02/18/2006

nuclear correlation[14,15] experiments have increasingly been playing an active role in structure solution of zeolitic materials. We have used ^{27}Al 3QMAS NMR and ^{27}Al−^{31}P heteronuclear correlation experiments to identify the number of T-sites in EMM-3 and understand their correlations, respectively.

Experimental Section

Synthesis of EMM-3. EMM-3 was prepared from reaction mixtures having the stoichiometry 0.5 $R(OH)_2$:Al_2O_3:P_2O_5:45 H_2O, where R is hexamethonium, $(CH_3)_3N(CH_2)_6N(CH_3)_3^{2+}$. In a typical synthesis, 85% H_3PO_4 (42.9 g, 0.213 mol of P_2O_5) was mixed with deionized water (56.9 mL, 3.16 mol) in a plastic beaker. Catapal A alumina (Condea Vista, 74% Al_2O_3, 29.4 g, 0.213 mol of Al_2O_3) was then mixed in with a spatula. This mixture was allowed to age at room temperature for 5 min and then mixed again for about 1 min with a spatula. (The aging step gives time for the alumina to react with the phosphoric acid to reduce the viscosity of the mixture and allow for better homogenization.) The hexamethonium dihydroxide template (Sachem, 22% aqueous, 114.5 g, 0.107 mol) was then added, and the mixture was transferred to a blender and vigorously mixed for an additional 5 min. Mixtures were heated in Teflon-lined autoclaves for 1−2 days at 150−200 °C. Products were recovered by centrifugation, slurried with water and recentrifuged four times to wash, and then dried at 115 °C in an air oven.

Characterization. Elemental analyses were performed by inductively coupled plasma atomic emission spectroscopy (ICP-AES) after Claise fusion digestion with lithium tetraborate/lithium carbonate flux. Gas adsorption was performed on an automated gas adsorption apparatus consisting of a Cahn vacuum microbalance with a MKS pressure manometer and controller. Calcined samples were heated overnight at 400 °C to a pressure $< 10^{-4}$ Torr before uptake measurements were performed at room temperature. Conventional powder X-ray diffraction with Bragg−Brentano geometry was measured on a Siemens D5000 diffractometer with Cu Kα radiation, a 1° divergent slit, and a step size of 0.02° 2θ. High-temperature X-ray diffraction with Bragg−Brentano geometry was measured on a Scintag XDS-2000 diffractometer equipped with an Edmund Bühler HDK 2.3 high-temperature X-ray chamber.

Selected area electron diffraction measurements were made at 200 kV on microcrystalline samples that had been first outgassed overnight in the column vacuum of the JEOL JEM 2010 electron microscope. Diffraction patterns were calibrated against a gold powder diffraction standard and were recorded on Kodak SO-163 electron microscope film (developed with Kodak HRP developer). Diffraction intensities were measured with the computer program ELD[16] after the patterns had been digitized on a flat-bed scanner. High-resolution digital electron microscope images obtained with a Philips CM200FEG instrument were recorded on a Gatan CCD camera and were analyzed by CRISP[17] image processing programs.

Solid-State NMR. ^{27}Al MAS NMR spectra were recorded at 11.7 T (Varian InfinityPlus 500) corresponding to ^{27}Al Larmor frequency of 130.1 MHz. The ^{27}Al MAS spectra were obtained with a $\pi/12$ rad pulse length and a recycle delay of 0.2 s. The ^{31}P MAS NMR spectra were recorded at 11.7 T corresponding to ^{31}P Larmor frequency of 202.1 MHz. The samples were loaded in MAS rotors and spun at the magic angle at rates of 10−16 kHz, and all measurements were done at room temperature. The ^{27}Al and ^{31}P chemical shifts are referenced with respect to external solutions of $Al(H_2O)_6^{3+}$ (δ_{Al} = 0.0 ppm) and 85% H_3PO_4 (δ_P = 0.0 ppm), respectively. The ^{31}P and ^{27}Al spectra were recorded on the as-synthesized, calcined/dehydrated (650 °C/3 h), and calcined/rehydrated samples. Rehydration of the calcined materials was done by exposing samples to a 100% relative humidity environment over a period of time, typically overnight. The solid-state ^{27}Al 3QMAS and MQ-selected ^{27}Al−^{31}P heteronuclear correlation (MQHETCOR) NMR spectra were recorded at 11.7 T on a Varian triple-resonance 4-mm T3 TR probe. The pulse sequence used for the MQMAS experiment was 3QMAS with *Z*-filter.

Synchrotron Powder X-ray Diffraction. A calcined/dehydrated sample of AlPO EMM-3 was sealed under vacuum at 300 °C in a 2.0 mm quartz capillary tube. The room-temperature synchrotron powder X-ray diffraction pattern was measured at beamline X-10B at Brookhaven National Laboratory at a wavelength of 0.871 43 Å from 3.5 to 60.0° 2θ and a step size of 0.005°. A focusing Ge (220) monochromator was used on the incident beam.

Results and Discussion

Synthesis. The use of organic amines and tetraalkylammonium cations to prepare aluminosilicate zeolites has been known for over 40 years.[18] These large organic cations, or SDAs, can induce the formation of new microporous frameworks. It is believed that these organics are the template around which the microporous cages and channels are formed during crystallization.[19] Many other factors, such as silica to alumina composition, inorganic cations, pH, nucleation, stirring, time, and temperature, also play a critical role in zeolite formation. In contrast to aluminosilicate zeolites, aluminophosphate syntheses are usually realized in a relatively narrow reactant gel composition range (Al_2O_3:1.0 ± 0.2 P_2O_5). While there are many aluminosilicate zeolites that can be prepared without organic templates, there are very few aluminophosphate materials that can be prepared without them. Therefore, a diversity of organic SDAs is critical to the discovery of new microporous aluminophosphate frameworks.

EMM-3 was synthesized from an aluminophosphate gel with the use of hexamethonium as the SDA at a temperature of 160 °C in 20 h with and without stirring. The X-ray diffraction pattern of EMM-3 shown in Figure 1 indicated that the sample was a new material. Attempts to index the diffraction pattern were unsuccessful, indicating that the material had low, possibly triclinic, symmetry. AlPO EMM-3 crystallizes in platelet morphology with dimensions of 0.5−2 μm by <0.05 μm thick as shown in Supporting Information.

Characterization of EMM-3. A sample of AlPO EMM-3 was calcined in air at 650 °C. After being cooled to room temperature in ambient air, this rehydrated material was

(11) Frydman, L.; Harwood, J. S. *J. Am. Chem. Soc.* **1995**, *117*, 5367.
(12) Madek, A.; Harwood, J. S.; Frydman, L. *J. Am. Chem. Soc.* **1995**, *117*, 12779.
(13) Fernandez, C.; Amoureux, J.-P.; Chezeau, J. M.; Delmotte, L.; Kessler, H. *Microporous Mater.* **1996**, *6*, 331.
(14) Fernandez, C.; Morais, C.; Rocha, J.; Pruski, M. *Solid State Nucl. Magn. Reson.* **2002**, *21*, 61.
(15) Amoureux; J.-P.; Pruski, M. In *Encyclopedia of Nuclear Magnetic Resonance, Vol. 9*; Grant, D. M., Harris, R. K., Eds.; John Wiley & Sons: Hoboken, NJ, 2002; p 226.
(16) Zou, X. D.; Sukharev, Y.; Hovmöller, S. *Ultramicroscopy* **1993**, *49*, 147.
(17) Hovmöller S. *Ultramicroscopy* **1992**, *41*, 121.
(18) Barrer, R. M.; Denny, P. J. *J. Chem. Soc*. **1961**, 971.
(19) Lok, B. M.; Cannan, T. R.; Messina, C. A. *Zeolites* **1983**, *3*, 282.

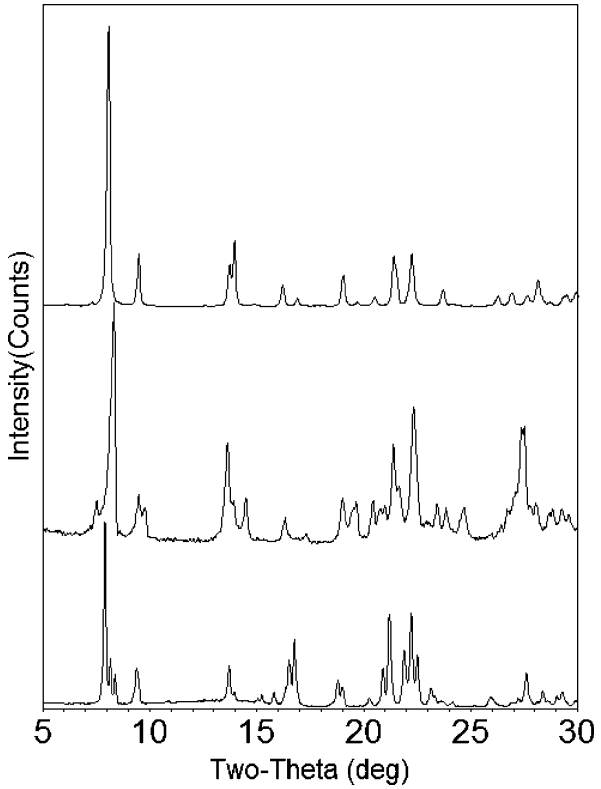

Figure 1. Powder X-ray diffractions patterns (Cu Kα) of EMM-3: as synthesized (lower); calcined/hydrated (middle); calcined/dehydrated (upper).

subjected to X-ray diffraction and shown to be crystalline, although the diffraction pattern has changed significantly from the as-synthesized material (see Figure 1). As before, the diffraction pattern could not be indexed. The high-temperature X-ray diffraction pattern of this calcined sample was measured at 153 °C in a flow of dry nitrogen. The diffraction pattern has changed significantly once more and is quite different from both the as-synthesized and calcined/hydrated forms. The X-ray diffraction pattern of the calcined/dehydrated form of EMM-3, as shown in Figure 1, has fewer lines, indicating a higher symmetry, and was easily indexed with an orthorhombic unit cell of dimensions $a = 10.3$ Å, $b = 12.6$ Å, and $c = 21.8$ Å. Systematic absences of reflections indicated that the space group was either *Imma* (no. 74), *Iba*2 (no. 45) or *Ima*2 (no. 46), or possibly *I*222 (23). This phenomenon of reversible diffraction pattern upon hydration and dehydration is indicative of changing symmetry due to hydration of the framework and is commonly seen in other aluminophosphate materials. While the idealized AlPO structures contain only 4-coordinate T-atoms, it is possible under certain conditions that some of the framework atoms may be 5- or 6-coordinate. This happens when some T-atoms become coordinated to one or two oxygen atoms of water molecules (-OH_2), or of hydroxyl groups (-OH). A good example is the molecular sieve $AlPO_4$-34, which is known to reversibly change the coordination of some aluminum T-atoms from 4-coordinate to 5- and 6-coordinate upon hydration. The as-synthesized and calcined/hydrated forms have low, triclinic symmetry, while the dehydrated form shows the typical high-symmetry, rhombohedral form of chabazite (CHA) as described by Tuel et al.[20]

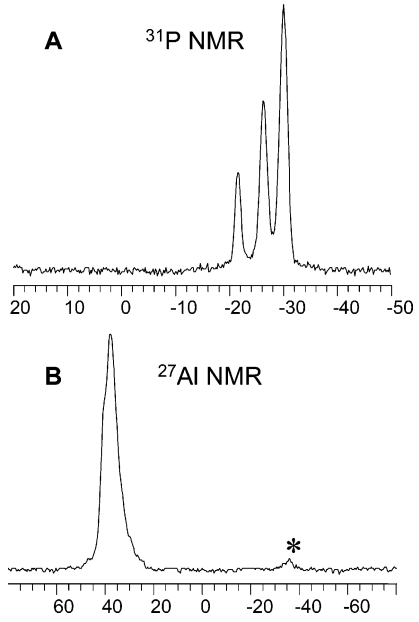

Figure 2. 202.1 MHz ^{31}P MAS NMR (A) and 130.1 MHz ^{27}Al MAS NMR (B) of calcined/dehydrated form of AlPO EMM-3. Asterisk indicates spinning side band.

Table 1. Adsorption of Hydrocarbons by Calcined AlPO EMM-3

absorbate	kinetic diameter (Å)	pressure, Torr	temp, °C	wt % uptake
methanol	3.8	40	20	12.8
n-hexane	4.3	50	25	10.3
cyclohexane	6.0	40	20	8.7
m-xylene	6.8	2.5	20	9.6

The adsorption of hydrocarbons was measured on a calcined sample of AlPO EMM-3. The adsorption capacity of 9−10 wt. % hydrocarbons is typical for a single-channel 12-ring zeolite (Table 1). The density of a calcined/dehydrated sample of AlPO EMM-3 was then carefully measured in a 1.863 cm^3 glass pycnometer using *m*-xylene to get an indication of the number of framework atoms in the unit cell. After correction for the *m*-xylene adsorption capacity of 9.6%, the density of AlPO EMM-3 was calculated to be 1.71 g/cm^3. This density and a unit cell volume of 2829 $Å^3$ (10.3 × 12.6 × 21.8 Å) represents a tetrahedral framework atom density of approximately 48 atoms/unit cell.

NMR gives valuable information on the local environment of the framework atoms and is often helpful for determining the total number of unique framework atoms. Figure 2 shows the ^{27}Al and ^{31}P MAS NMR spectra recorded at 11.7 T. Although ^{27}Al NMR spectra are usually complicated due to unresolved quadrupolar broadening, the resonances of the calcined/dehydrated form centered around 37−40 ppm indicate only T_d coordination and that the framework has a fully connected, three-dimensional structure. The ^{31}P NMR of the calcined/dehydrated form shows three resonances at −22, −27, and −30 ppm with a ratio of intensity of 1:2:3, respectively. This suggests that the space group symmetry for the unit cell of calcined EMM-3 must account for a minimum of three, or a multiple of three, crystallographic T sites in the ratio of 1:2:3. As determined from the density

(20) Tuel, A.; Caldarelli, S.; Meden, A.; McCusker, L. B.; Baerlocher, Ch.; Ristic, A.; Rajic, N.; Mali, G.; Kaucic, V. *J. Phys. Chem. B* **2000**, *104*, 5697.

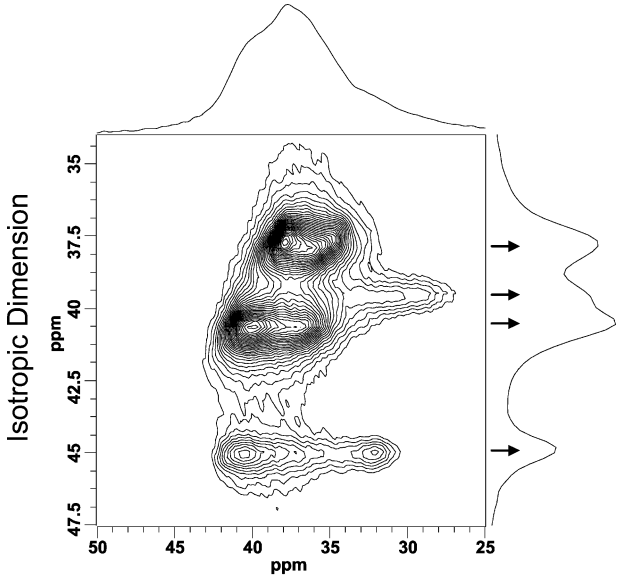

Figure 3. 130.1 MHz ^{27}Al 3QMAS NMR of AlPO EMM-3 at 13.3 kHz MAS of calcined/dehydrated form of EMM-3 showing the presence of *four* peaks in the isotropic dimension (arrows), indicating at least *four* crystallographically distinct T_d environments for ^{27}Al.

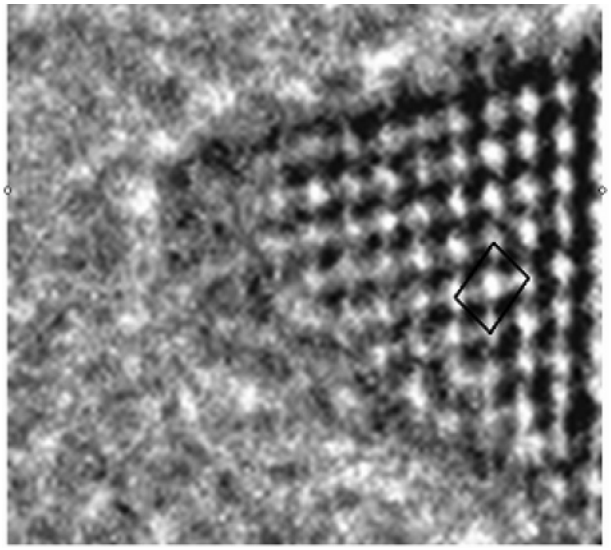

Figure 4. HREM of EMM-3 showing channel pores down the [100] direction. The box shows the unit cell and appears nonorthogonal due to a slight tilt of the crystal.

and unit cell volume, the EMM-3 structure contains 48 T-atoms. Therefore, the three ^{31}P peaks with a relative intensity of 1:2:3 correspond to 8, 16, and 24 T-atoms for a total of 48. The space group, *Imma*, has a general site multiplicity of 16, and a special position multiplicity of 8 for atoms on mirror planes or a 2-fold axis, and a special position multiplicity of 4 for atoms on both mirror planes and a 2-fold axis.[21] Since the ^{31}P NMR spectrum does not show peaks of equal intensity, 1:1:1, corresponding to three unique atoms being on general positions ($3 \times 16 = 48$), some combination of atoms on both general and special positions must account for the relative intensity ratio of 1:2:3. In the simplest case, the ^{31}P peak with a relative intensity of 1 could correspond to one atom on a special position, either a mirror plane or 2-fold axis. The ^{31}P peak with a relative intensity of 2 could correspond to one atom on a general position, and the third ^{31}P peak with a relative intensity of 3 could correspond to one atom on a general position and one atom on a special position, either a mirror plane or 2-fold axis. Therefore, the structure of EMM-3 must have at least four unique atoms. Other combinations are also possible, such as one atom on a general position (multiplicity = 16) and four atoms on special positions (multiplicity = 8), and so on. The two other possible space groups, *Ima*2 and *Iba*2, have a general site multiplicity of 8 and a special position multiplicity of 4, so that the total number of unique atoms would be double if EMM-3 had either of these symmetries.

The ^{27}Al 3QMAS NMR spectrum of the calcined/dehydrated form of AlPO EMM-3 is shown in Figure 3. The 3QMAS NMR spectrum shows evidence of the presence of *four* isotropic peaks (indicated by arrows) in EMM-3, indicating at least *four* distinct T_d environments for ^{27}Al. The improvement in resolution in the isotropic dimension of the 3QMAS NMR data is a manifestation of the removal of the residual quadrupolar broadening. The detection of these four sites of ^{27}Al is a unique insight obtained from the 3QMAS NMR that was *not* observed in the 1D ^{27}Al MAS NMR spectra; even at ultrahigh field, no more than two T_d peaks could be identified.[22]

Structure Determination and Refinement. The determination of crystal structures from powder X-ray diffraction data remains a difficult task since the three-dimensional data from a single crystal is reduced to the one-dimensional data of the powder experiment. This results in severe overlap of peaks and the loss of valuable data. This is particularly true for orthorhombic EMM-3, which is dimensionally pseudohexagonal down the [100] axis. For EMM-3 there is severe overlap of peaks in the diffraction pattern, especially in the critical low-angle region. The first two reflections, (011) and (020), are completely overlapped, and down to a resolution of 1.5 Å about 60% of the peaks are overlapped.

In principle, electron diffraction intensity data would be useful for determining zonal structures.[23,24] Unfortunately, the most informative projection down the [100] axis was too thick so that the intensity data, due to multiple scattering perturbations,[25] could not be used for a quantitative structure analysis. However, observed plane group symmetries of three orthogonal zonal electron diffraction patterns reduced the number of possible space groups from four to two. Channel openings could be discerned from electron microscope lattice images for crystallites oriented along the [100] direction (Figure 4).

Grosse-Kuntsleve et al.[26] have developed a method of solving crystal structures from powder diffraction data, which

(21) *International Tables for Crystallography*, 4th ed.; Hahn, T., Ed.; Kluwer Academic Publishers: Boston, MA, 1996.

(22) Afeworki, M.; Kennedy, G. J.; Dorset, D. L.; Strohmaier, K. G. Synthesis and Characterization of a New Microporous Material. 2. AlPO and SAPO Forms of EMM-3. *Chem. Mater.* **2005**, *6*, 1705.

(23) Nicolopoulos, S.; Gonzalez-Calbet, J. M.; Vallet-Regi, M.; Corma, A.; Corell, C.; Guil, J. M.; Perez- Pariente, J. *J. Am. Chem. Soc*. **1995**, *117*, 8947.

(24) Dorset, D. L. *Z. Kristallogr*. **2003**, *218*, 458.

(25) Dorset, D. L. *Structural Electron Crystallography*; Plenum: New York, 1995.

Table 2. Results of DLS Refinement of the EMM-3 FOCUS Model[a]

model	space group	refinement	*a* (Å)	*b* (Å)	*c* (Å)	α (deg)	R_{DLS}
Si EMM-3	*Imma*	no unit cell	10.308	12.699	21.854	90.00	0.0020
Si EMM-3	*Imma*	unit cell	10.312	12.709	21.925	90.00	0.0016
AlPO EMM-3	*I*2/*m*11	no unit cell	10.308	12.699	21.854	90.00	0.0048
AlPO EMM-3	*I*2/*m*11	unit cell	10.48	12.93	22.15	89.62	0.0016

[a] $\beta, \gamma = 90.00°$. Prescribed distances and angles: $d_{Si-O} = 1.623$ Å, $d_{P-O} = 1.538$ Å, $d_{Al-O} = 1.748$ Å, $\text{angle}_{O-T-O} = 109.47°$, $\text{angle}_{T-O-T} = 145°$ using the weights of $W_{dT-O} = 2.0$, $W_{\text{angle}O-T-O} = 1.0$, and $W_{\text{angle}T-O-T} = 0.1$.

has been optimized for zeolite frameworks. The FOCUS program uses direct methods with Fourier recycling and a specialized zeolite topology search. The program GSAS[27] was first used to extract the peak intensities from the synchrotron powder X-ray diffraction data by the LeBail method. These data were then input to the FOCUS program, which gave a trial lattice with five unique T-atoms in short time with a FobsScale factor of 0.15. The FOCUS input file that gave this model is given in the Supporting Information.

The output of the FOCUS run gave the coordinates of the T-atoms. By use of the MSI Cerius2 modeling software package, framework oxygen atoms were placed at midpoints between the T-atoms and the model subjected to DLS refinement[28] to optimize the atomic coordinates to match those of known zeolite frameworks. Since this model is for an all-silica framework, a second model was created in which alternating aluminum and phosphorus atoms were placed into the unit cell. This lowers the symmetry to the monoclinic space group *I*2/*m*11 (no. 12). This model was also subjected to DLS refinement. Using interatomic distances of Si−O = 1.62 Å, Al−O = 1.75 Å, and P−O = 1.54 Å, four models were optimized. Two models were refined, constraining the unit cell dimensions to those measured from the synchrotron data, $a = 10.308$, $b = 12.699$, and $c = 21.854$ Å, and two models were refined with no unit cell restraints. With no unit cell restraints, the refinements gave cell dimensions very close to the experimental values as shown in Table 2. All four refinements gave reasonable models with low R_{DLS} values (<0.005), indicating that the proposed framework is feasible.

The DLS refined atomic positions from the monoclinic AlPO model were then used as starting coordinates for Rietveld refinement of the synchrotron powder X-ray data by use of the program GSAS.[27] A shifted Chebyshev[29] function with 20 parameters was used to fit the background, and a seven-parameter pseudo-Voigt function[30] was used to fit the peak profile. The framework tetrahedral atoms and oxygen atoms were constrained to have the same isotropic thermal parameters. Soft restraints were placed on the Al−O (1.745 ± 0.02 Å), P−O (1.535 ± 0.05 Å), and the tetrahedral oxygen−oxygen distances (2.85 ± 0.05 and 2.51 ± 0.05 Å). Although the relative weight of these restraints could be reduced throughout the refinement, they could not be fully removed and a final soft restraint weight factor of 100 was used. Complete removal of these restraints led to some unreasonable interatomic distances and only reduced the R_{wp} factor from 7.0% to 6.9%. There were 11 396 total observations including 97 soft restraints with a total of 96 refinable variables. The final agreement factors were $R_{wp} = 7.0\%$ and expected $R_{wp} = 1.5\%$ (see Table 3).

Table 3. Crystallographic Refinement Data for EMM-3

molecular formula	$Al_{24}P_{24}O_{96}$
formula weight	2929.9
a	10.3132(2) Å
b	12.6975(3) Å
c	21.8660(4) Å
α	89.656(1)°
V	2866.0(1) Å^3
Z	1
space group	*I*2/*m*11 (no. 12)[a]
T	25 °C
λ	0.87143 Å
N_{obs}	11 299
R_p[b]	5.38%
R_F^2	3.8%
χ^2	22.4%
R_{wp}	7.00%
expected R_{wp}	1.5%

[a] Unique axis *a*, cell choice 3. [b] $R_{wp} = \{\Sigma w(I_o - I_c)^2/\Sigma w I_o^2\}^{1/2}$; $R_p = \Sigma|I_o - I_c|/\Sigma I_o$; $\chi^2 = \Sigma w(I_o - I_c)^2/N_{obs} - N_{var}$; expected $R_{wp} = R_{wp}/\{\chi^2\}^{1/2}$. I_o = observed intensity of each point; I_c = calculated intensity of each point.

The highest framework symmetry is the orthorhombic space group *Imma*, which would be expected for an all-silica framework. As discussed above, alternation of aluminum and phosphorus atoms in the AlPO framework removes a mirror plane and a glide plane to lower the symmetry to the monoclinic space group *I*2/*m*11. Therefore, two refinements were performed, both with and without constraining the α unit cell angle to 90.00° to determine if it is truly orthogonal. The model fit improved significantly when α was allowed to refine to 89.66° as indicated by the R_{wp} factor decreasing from 12.2% to 7.0%. Although it is difficult to see any indication in the X-ray diffraction (XRD) pattern of a monoclinic cell, one section of the XRD pattern clearly shows an α shift. At 18.8° 2θ, the orthogonal cell has one reflection, (136), while the cell with $\alpha = 89.66°$ has three allowed reflections, (136), (−1,3,6), and (330). There are clearly at least two visible peaks in this region, verifying the nonorthogonal angle (see Supporting Information).

Final atomic coordinates and thermal parameters (with estimated standard deviations) are given in Table 4, and the comparison of the calculated and observed X-ray diffraction patterns is shown in Figure 5. The final interatomic distances and angles are given in the Supporting Information, although it is noted that these values reflect the soft restraints used in the refinement. Nonetheless, the final results are consistent with other known framework structures, the agreement values are very good, and the simulated XRD pattern closely matches the experimental data.

Description of the Structure of EMM-3. The unit cell of EMM-3 contains five unique T-atoms in the ideal framework. Three atoms are located on mirror planes, one

(26) Grosse-Kuntsleve, R. W.; McCusker, L. B.; Baerlocher, Ch. *J. Appl. Crystallogr.* **1997**, *30*, 985.
(27) Larson, A. C.; VonDreele, R. B. GSAS: General Analysis Structural System; Los Alamos National Laboratory: Los Alamos, NM, 2000.
(28) Baerlocher, Ch.; Hepp, A.; Meier, W. M. *DLS-76, A Program for the Simulation of Crystal Structrues by Geometric Refinement*; Institute of Cryst and Petrography: Zürich, Switzerland, 1977.
(29) *Handbook of Mathematical Functions*; Stegun, I. A., Abramawitz, M., Eds.; U.S. Government Printing Office: Washington, DC, 1972.
(30) Thompson, P.; Cox, D. E.; Hastings, J. B. *J. Appl. Crystallogr.* **1987**, *20*, 79.

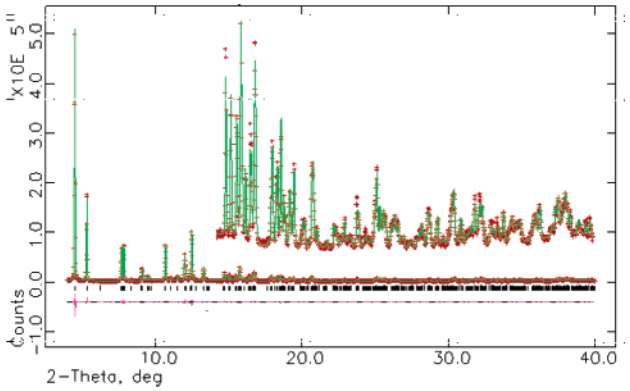

Figure 5. Final plot of synchrotron data showing experimental intensity (+), calculated intensity (−), and difference curve (lower). Tic marks indicate allowed reflections, and the inset is intensity ×20.

atom on a 2-fold axis and another in a general position. In the AlPO form, there are 10 unique T -atoms: three P and three Al on mirror planes, one P and one Al atom on a 2-fold axis, and another P and Al in general positions. This is in agreement with the ^{31}P NMR, which shows three resonances of relative intensity of 1:2:3. It is not possible from 1D NMR to determine whether the peak with a relative intensity of 2 is due to two T-atoms on special positions or one atom on the general position. However, the 2D ^{27}Al → ^{31}P MQHETCOR spectrum discussed below indicates that the 1D ^{31}P MAS spectral intensities are due to the overlap of five peaks of relative intensity 1:2:1:1:1 [i.e., 1:2:(1:1:1)].

Figure 6 shows the 2D ^{27}Al → ^{31}P 3QHETCOR spectrum of EMM-3 on the left side and slices from the contours displayed on the right side of the 2D spectra map out the Al−P correlations. MQ-HETCOR spectra have been shown to provide an additional degree of freedom and help in establishing sites that are generally indistinguishable in 1D MAS NMR spectra.[15,31] Due to the narrow chemical shift range of the various T-sites, the 3Q-HETCOR spectrum of

Table 4. Final Atomic Positions of EMM-3 from Rietveld Refinement[a]

atom	site	*x*	*y*	*z*	occupancy	U_{iso}(Å)
Al1	8 j	0.2247(5)	0.3744(4)	0.1119(2)	1	0.0119(4)
Al2	4 i	0.0000	0.5563(5)	0.6544(3)	1	0.0119(4)
Al3	4 i	0.0000	0.8722(5)	0.7949(3)	1	0.0119(4)
Al4	4 i	0.0000	0.8762(5)	0.4341(3)	1	0.0119(4)
Al5	4 h	0.2190(7)	0.5000	0.5000	1	0.0119(4)
P6	8 j	0.7784(5)	0.1322(4)	0.1118(2)	1	0.0119(4)
P7	4 i	0.0000	0.6216(5)	0.7918(3)	1	0.0119(4)
P8	4 i	0.0000	0.6292(5)	0.4322(3)	1	0.0119(4)
P9	4 i	0.0000	0.9457(4)	0.6603(3)	1	0.0119(4)
P10	4 h	0.7767(6)	0.0000	0.5000	1	0.0119(4)
O11	4 i	0.0000	0.5584(8)	0.7332(3)	1	0.0110(7)
O12	4 i	0.0000	0.7391(6)	0.7734(4)	1	0.0110(7)
O13	4 i	0.0000	0.5766(6)	0.3683(4)	1	0.0110(7)
O14	4 i	0.0000	0.7454(6)	0.4179(4)	1	0.0110(7)
O15	8 j	0.1950(5)	0.7550(5)	0.9103(3)	1	0.0110(7)
O16	4 i	0.0000	0.9520(8)	0.7294(3)	1	0.0110(7)
O17	4 i	0.0000	0.9430(6)	0.3667(4)	1	0.0110(7)
O18	8 j	0.1984(7)	0.4528(6)	0.0511(3)	1	0.0110(7)
O19	8 j	0.1196(6)	0.4071(6)	0.1717(3)	1	0.0110(7)
O20	8 j	0.3813(5)	0.3856(6)	0.1389(3)	1	0.0110(7)
O21	8 j	0.8785(5)	0.4039(5)	0.5349(3)	1	0.0110(7)
O22	8 j	0.8097(8)	0.0611(6)	0.0570(3)	1	0.0110(7)
O23	8 j	0.8573(6)	0.1001(6)	0.1666(3)	1	0.0110(7)
O24	8 j	0.6346(5)	0.1171(6)	0.1242(4)	1	0.0110(7)
O25	8 j	0.1348(5)	0.0904(5)	0.5230(4)	1	0.0110(7)

[a] Estimated standard deviations are in parentheses.

EMM-3 is a lot more complicated than that of $AlPO_4$-14. Nevertheless, attempts were made to verify the five distinct sites observed from the structure. The projection on to the ^{27}Al dimension shows similar resolution to the isotropic projection of the ^{27}Al 3QMAS data (Figure 3). However, the dipolar couplings with ^{31}P add another dimension to these data that offer the possibility of higher resolution by mapping out the Al−P connectivities. Close inspection of the correlations indicate that the peak with relative intensity of 3 centered at $\delta_P \sim -30$ ppm in the 1D ^{31}P MAS spectrum is composed of three overlapping peaks and the peak centered at $\delta_P \sim -26$ ppm with relative intensity of 2 is a single

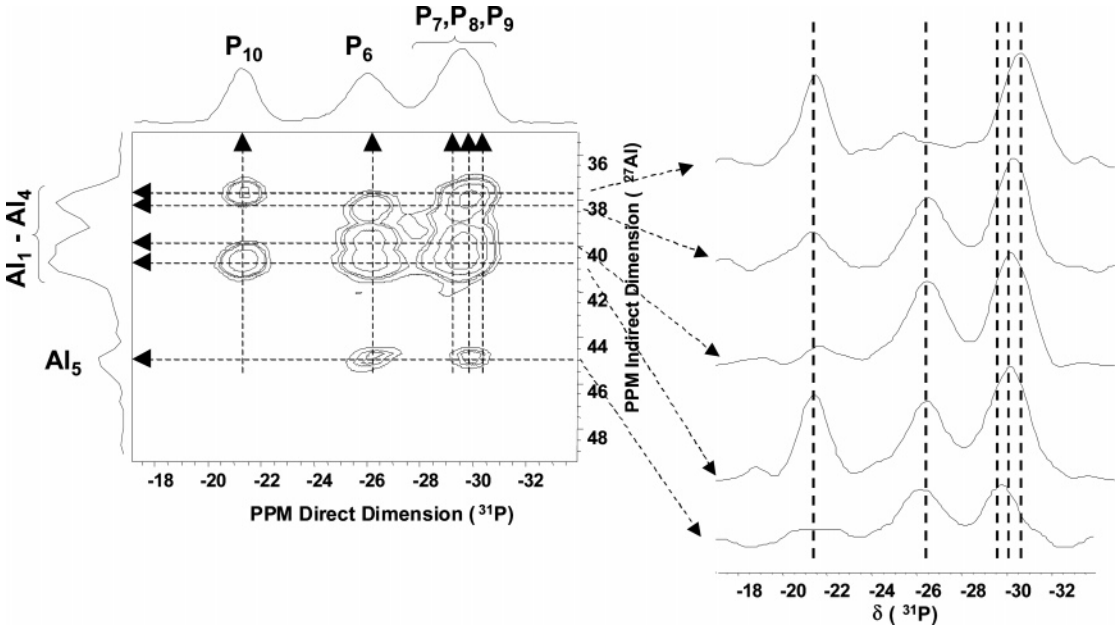

Figure 6. MQ-selected Al−P HetCor NMR of calcined/dehydrated form of AlPO EMM-3: ^{27}Al → ^{31}P 3QHETCOR MAS NMR at 10 kHz MAS of EMM-3. The cross-sections in the ^{31}P MAS dimension, that is, slices from the contours, are displayed on the right side of the 2D spectra. These cross sections map out the Al−P correlations. Vertical lines on the spectral slices indicate multiple resonances within the same broad peak. Tentative peak assignments are included. Horizontal and vertical dashed lines through the center of the contours are shown as a guide to the eye.

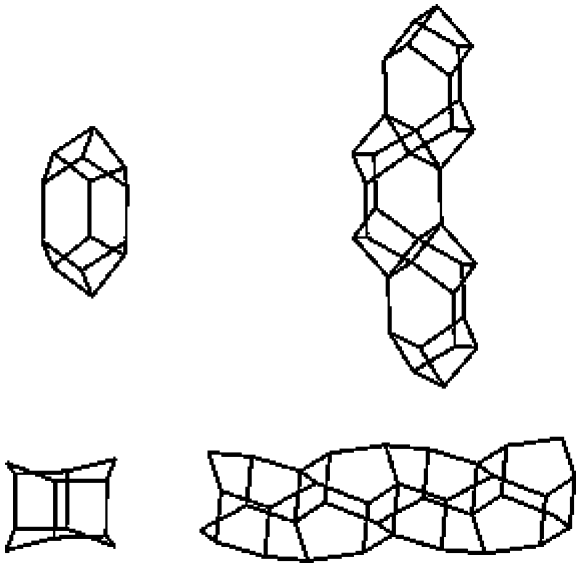

Figure 7. Secondary building units of EMM-3. Upper, capped six rings; lower, open D6R. The right side shows the way they are connected to form unique chains not seen previously in other frameworks. Oxygen atoms are omitted for clarity.

peak (see vertical dashed lines in the slices selected). In a similar fashion, the P−Al correlations mapped out on to the ^{27}Al dimension suggest that the peak at $\delta_{Al} \sim 38$ ppm in the ^{27}Al projection is actually composed of two peaks as indicated by the horizontal dashed lines. Similarly, the peak at $\delta_{Al} \sim 40$ ppm in the ^{27}Al projection appears to be composed of two sites. Thus, with the additional degree of freedom provided by the ^{31}P dimension in the MQ-HETCOR experiment there is evidence of the presence of up to *five* isotropic peaks in EMM-3, indicating five distinct T_d environments for Al and P, respectively. By use of the observed peak areas in the 1D MAS spectra, the correlations in the 2D MQHETCOR data, and the expected T−O−T connectivities (Supporting Infomation), it is possible to make some tentative spectral assignments. One of the five distinct T_d P and Al atoms (i.e., P_6 and Al_1) is expected to have twice the population relative to the other four atoms. The observed ^{31}P peak areas and the P−O−Al correlations suggest that the peak at $\delta_P \sim -26$ ppm of relative intensity 2 can be assigned to P_6. The peak at $\delta_P \sim -21$ ppm that shows only two P−O−Al correlations is assigned to P_{10}. By elimination, the peak at $\delta_P \sim -30$ ppm of intensity 3 is assigned to the overlap of peaks from P_7, P_8, and P_9. Similarly, the peak at $\delta_{Al} \sim 45$ ppm that shows only two P−O−Al correlations is assigned to Al_5 and the four overlapping peaks at $\delta_{Al} \sim 37-41$ ppm are assigned to Al_1, Al_2, Al_3, and Al_4.

The framework is built from double 6-rings (D6Rs) secondary building units (SBUs) that are open at opposite ends, having the face symbol $6^4 4^2$ (a polyhedron containing four 6-rings and two 4-rings), and connected to one another to form unique chains along the *a*-axis, [100] direction. Although these open D6Rs are present in the ATO, DFO, IFR, OSI, and SAO frameworks,[4] the manner in which they are connected has not been observed before (Figure 7). These chains are connected together by capped 6-ring polyhedron, having the face symbol $6^3 4^6$ that run along the *b*-axis, [010] direction. Capped 6-ring SBUs are present in the BPH and AFS frameworks,[4] and are connected by sharing vertexes. In EMM-3 the capped 6-rings are connected by sharing faces to form unique chains, which have not been observed previously (Figure 7).

The capped 6-rings and open D6R secondary building units in EMM-3 form a new framework that has single-channel 12-member rings along the [100] direction as shown in Figure 8. These channels are elliptical in shape and are

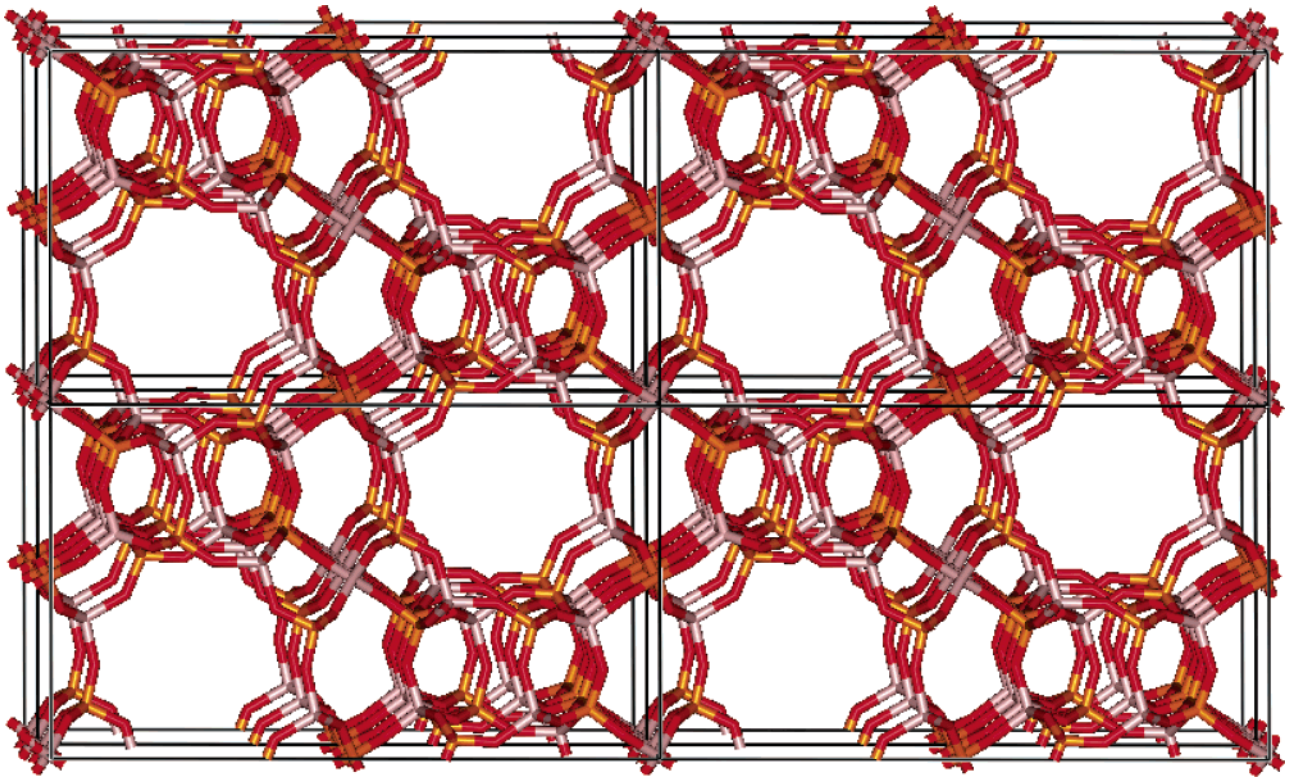

Figure 8. View of the refined structure of AlPO EMM-3 down the [100].

sinusoidal (see Supporting Information). The shape of the 12-member ring channel is rather complex as there are 13 unique 12-ring pores along the channel. The size of the opening is about 6.1 × 6.5 Å depending on which 12-ring pore is measured. (The pore size is determined by measuring the distance between centers of oxygen atoms across the ring and subtracting the van derWaals oxygen diameter of 2.7 Å.) Along the [010] direction are highly elliptical 8-ring channels with an opening of 1.2 × 5 Å. These 8-ring pores are connected to the 12-ring channels in a way such that they also run along the [001] direction in a sinusoidal manner. EMM-3 can therefore be described as a 12 × 8 × 8-ring framework.

Conclusion

EMM-3 is a new microporous material that can be prepared from an aluminophosphate gel containing hexamethonium as a template at 160 °C in 20 h. It is stable to calcination in air and absorbs 9−10 wt % hydrocarbons. The structure of EMM-3 has been solved by use of the program FOCUS, and the structure was refined from powder data by use of synchrotron X-ray radiation. The unit cell for the calcined AlPO form of EMM-3 has monoclinic space group symmetry, *I*2/*m*11, with the cell dimensions $a = 10.3132(2)$, $b = 12.6975(3)$, and $c = 21.8660(4)$ and $\alpha = 89.656(1)°$. The structure is microporous and contains 12-ring, unidimensional channels with pore openings of 6.1 × 6.5 Å. This new framework is built from open double 6-ring and capped 6-ring polyhedra secondary building units connected to form two new building chains, not observed in other known frameworks. The ^{31}P and ^{27}Al NMR spectra of the calcined/dehydrated form are in agreement with a fully connected tetrahedral structure containing five unique phosphorus and five unique aluminum atoms.

Acknowledgment. We thank Arthur W. Chester, William Borghard, and William Harrison for assistance and thoughtful discussions, as well as Mark Disko for assistance in obtaining electron microscope lattice images. B. Liang and C. E. Chase recorded the NMR spectra at 11.7 and 8.4 T, respectively, and Stephen Bennett recorded the synchrotron X-ray diffraction pattern. We are grateful to Dr. Christian Fernandez, Université de Caen, France, for a sample of $AlPO_4$-14 that was used as a setup sample for 3QMAS NMR experiments. The help of Dr. J. Frye, Varian Inc., in setting up the initial stages of the MQMAS and HETCOR experiments is gratefully acknowledged. The authors thank ExxonMobil Research and Engineering Company for research support and for being able to publish this material.

Supporting Information Available: FOCUS input file, graph of section of PXD pattern showing monoclinic shift, final interatomic distances and angles, figure of 12-ring channel of EMM-3 ([010] direction) showing the 8-ring pores, table of powder diffraction data of calcined/dehydrated EMM-3, figure of 12-ring channel showing the sinusoidal channels, and scanning electron micrograph, and two X-ray crystallographic files (CIF), one with unique axis *a* coordinates and another with unique axis *b* coordinates. This material is available free of charge via the Internet at http://pubs.acs.org.

CM052174R

(31) Roux, M.; Marichal, C.; Paillaud, J.-L.; Fernandez, C.; Baerlocher, Ch.; Chezeau, J.-M. *J. Phys. Chem. B* **2001**, *105*, 9083.